Supporting Information

Furic et al. 10.1073/pnas.1005320107

SI Materials and Methods

Cloning of the eIF4E^{S209A} Targeting Vector. The KI DNA construct was built using amplified fragments of genomic DNA. The construct contained the serine 209 to alanine mutation in exon 8 and a Neo-TK selection cassette flanked by Frt sites within intron 7. The backbone vector, plox/frt, was previously described (1). The left flank was PCR amplified with the primers 5′-CCATTGTGGAATGCCCTAGGCC-3′ and 5′-CGTTATAGGCGCGCCATGGGCTCACAGCAATTGC-3′ and then digested and ligated into the AvrII and AscI sites of the backbone vector. The right flank, which contains the point mutation, was amplified in three fragments. The first fragment (A) was amplified with primer pair 5′-GCCGCCGGTTTAAACTGATCGTGATTTGCTTGTTAC-3′ and 5′-CCTATTTTTAGTGGTGGCGCCGCTCTTTGTAGC-3′, digested with PmeI and NarI. The second fragment (B) was amplified with the primer pair 5′-GCTACAAAGAGCGGCGCCACCACTAAAAATAGG-3′ and 5′-CCACAATTATGTTTAGGGATC-3′ and then digested with NarI and HindIII. Fragments A and B were inserted into the PmeI/HindIII sites of the backbone vector by triple ligation. The third fragment (C) was amplified with the primer pair 5′-GCTCCACTCCATGCAGGAGCGG-3′ and 5′-CGCAGAGGTCGACTTGCCCCATAATACTCCAC-3′, digested with HindIII and SalI and ligated into the HindIII/SalI sites of the vector already containing fragments A and B. The entire right flank was digested with PmeI and SalI and ligated into PmeI/SalI sites of the left flank containing construct to generate p-eIF4E-KI S209A.

ES Cell Selection. p-eIF4E-KI S209A plasmid DNA was linearized with SalI and electroporated in 129Sv/J ES cells and selection of G418 resistant transformants was done as previously described (2). A total of 480 G418 resistant colonies were tested for recombination by Southern blotting.

Polysome Microarray Analysis. WT and KI MEFs (5×10^6 cells) were grown in DMEM supplemented with 10% FBS. Polysomal and total cytoplasmic RNA was isolated as described (3). Fractions containing mRNAs bound to more than three ribosomes were pooled and designated heavy polysomal RNA. RNA isolation was performed in two independent experiments from one pair of KI and WT MEFs. RNA quality was assessed using the Bioanalyzer Nano-Chip (Agilent), and all RNA samples were of good quality (integrity number, > 9.6). RNA (250 ng) was labeled using the one-cycle Illumina protocol and the resulting cRNA was hybridized with the "MouseRef-8_V2" BeadChip (Illumina). Data analysis was performed using the statistical environment R and the package lumi (4). Data were transformed using Variance Stabilizing Transformation and normalized using Robust Spline Normalization. Technical quality was validated and biological quality was assessed using principal components analysis, which showed good separation of the WT and the KI samples, for both the heavy polysome RNA data and the heavy polysome RNA data corrected for cytosolic RNA levels, in the first component. Correction for cytosolic RNA was performed by subtracting the log2 mean cytosolic RNA levels from the corresponding polysome RNA levels. Identification of differentially expressed genes was done using Significance Analysis of Microarrays algorithm (5). Genes that were significant ($q < 15$) before and after correction for the cytosolic RNA level were collected. Microarray data were deposited in the Gene Expression Omnibus database (accession no. GSE17451).

Immunoreactivity Quantification and Statistical Analysis of Human Prostate Tissue. The immunoreactivity scoring was performed by an experimenter blinded to the grade of the lesions. Scoring procedure was done as follows: each core was scored according to the staining intensity (value of 0 for absence, 1 for weak, 2 for moderate, 3 for strong staining, and 4 for very strong staining). The nonparametric Kruskal-Wallis test was used to evaluate the differences between the intensity means of the normal, normal adjacent, PIN, HS tumor, and HR tumor tissues. The mean intensity of Gleason scores (≤ 7 and >7) was also compared by Mann–Whitney *U* test. The nonparametric Spearman rho correlation test was used to conduct correlation analysis. All statistical tests were performed using SPSS software, version 12 (SPSS).

Statistical Analysis of Mouse Prostate Tissue. Prostate tumor sections were stained with H&E and analyzed by two histopathologists blinded to the genotype of the mice. Lesions were graded from PIN I to PIN IV and invasive. A scoring procedure was done as follows: lesions were graded from 1 (PIN I) to 5 (invasive) and the weighted average was calculated for each section by taking into account the percentage of each lesion type on the section. The global score of each mouse was calculated by averaging the score of every slides corresponding to a single mouse. The nonparametric Mann–Whitney *U* test was used to evaluate the differences between the WT and KI cohorts.

Cell Cycle Analysis. Cells were lysed with NPE NIM-DAPI reagent (Beckman Coulter) and analyzed by using a Cell Lab Quanta SC (Beckman Coulter) flow cytometer.

Isolation of MEFs. MEFs were isolated from 14.5-d pregnant females as previously described (6). Animal protocols were approved by the McGill University Animal Care Committee and in compliance with McGill University guidelines.

Orthophosphate Labeling. eIF4E was immunoprecipitated from $H_3{}^{32}PO_4$ metabolically labeled MEFs as previously described (7).

Mouse Tissue Processing. Mouse urogenital system was isolated en bloc and fixed for 24 h in 10% buffered formalin. Alternatively, one half of the urogenital system was dissected to isolate the ventral, anterior, and dorsolateral lobes of the prostate. Tissues were paraffin-embedded, and 5-μm sections were used for H&E staining and IHC.

shRNA-Mediated Knockdown of RAPTOR. shRNA vectors (RAPTOR 1857 and Scrambled 1864; 7 μg; Addgene) were cotransfected into HEK293T cells in 100-mm dishes with lentivirus packaging plasmids PLP1, PLP2, and PLP-VSVG (7 μg of each; Invitrogen) using Lipofectamine 2000 (Invitrogen). Supernatant was collected 48 h and 72 h after transfection, passed through a 0.45-μm nitrocellulose filter, and applied on target cells with Polybrene (5 μg/mL). Cells were reinfected the next day and selected with puromycin for 48 h (1 μg/mL; Sigma).

Apoptosis Induction. Subconfluent layers of MEFs were treated with ionomycin for 24 h. Annexin V and PI staining was performed using Annexin-V-FLUOS staining kit (Roche Diagnostics) according to the manufacturer's instructions. The percentage of apoptotic and necrotic cells was determined as described (8).

Patient Cohort and TMA Construction. The TMA used for IHC was previously described (9, 10). Briefly, the specimen cohort, consisting

of 601 one-mm-wide cores of prostate tissue, was used for IHC studies. The TMA was constructed with cores representing 43 patients with normal prostate tissues, 62 patients presenting primary PCa tissues, and 30 patients with HR PCa, for a total of 135 patients.

1. Brown EJ, Baltimore D (2003) Essential and dispensable roles of ATR in cell cycle arrest and genome maintenance. *Genes Dev* 17:615–628.
2. Ramírez-Solis R, Davis AC, Bradley A (1993) Gene targeting in embryonic stem cells. *Methods Enzymol* 225:855–878.
3. Larsson O, et al. (2007) Eukaryotic translation initiation factor 4E induced progression of primary human mammary epithelial cells along the cancer pathway is associated with targeted translational deregulation of oncogenic drivers and inhibitors. *Cancer Res* 67:6814–6824.
4. Du P, Kibbe WA, Lin SM (2008) lumi: A pipeline for processing Illumina microarray. *Bioinformatics* 24:1547–1548.
5. Tusher VG, Tibshirani R, Chu G (2001) Significance analysis of microarrays applied to the ionizing radiation response. *Proc Natl Acad Sci USA* 98:5116–5121.
6. Le Bacquer O, et al. (2007) Elevated sensitivity to diet-induced obesity and insulin resistance in mice lacking 4E-BP1 and 4E-BP2. *J Clin Invest* 117:387–396.
7. Frederickson RM, Montine KS, Sonenberg N (1991) Phosphorylation of eukaryotic translation initiation factor 4E is increased in Src-transformed cell lines. *Mol Cell Biol* 11:2896–2900.
8. Miller E (2004) Apoptosis measurement by annexin v staining. *Methods Mol Med* 88: 191–202.
9. Le Page C, Koumakpayi IH, Alam-Fahmy M, Mes-Masson AM, Saad F (2006) Expression and localisation of Akt-1, Akt-2 and Akt-3 correlate with clinical outcome of prostate cancer patients. *Br J Cancer* 94:1906–1912.
10. Diallo JS, et al. (2007) NOXA and PUMA expression add to clinical markers in predicting biochemical recurrence of prostate cancer patients in a survival tree model. *Clin Cancer Res* 13:7044–7052.

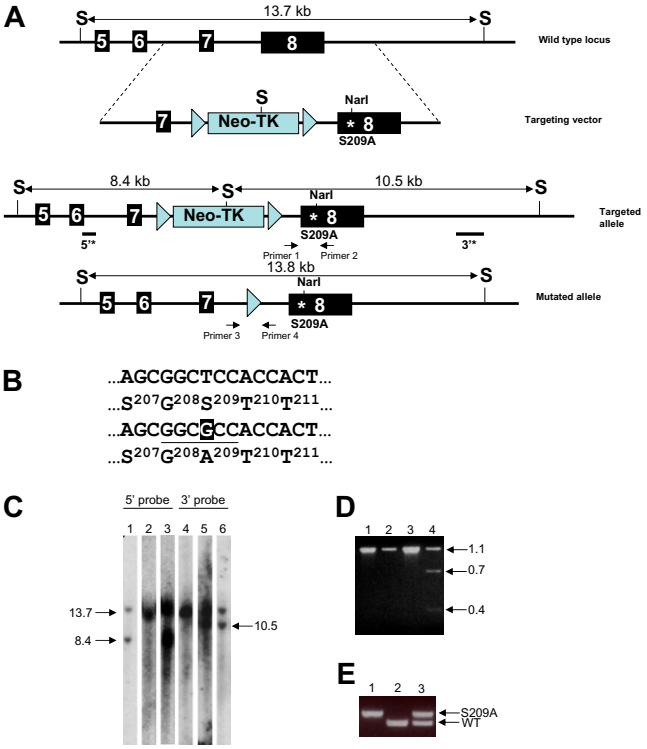

Fig. S1. Generation of a KI mouse expressing non phosphorylatable eIF4E. (*A*) A targeting vector containing the genomic DNA encompassing exons 7 and 8 of mouse eIF4E was used to introduce the mutated serine 209 into the eIF4E locus (S, SacI restriction site). (*B*) The introduction of a single nucleotide mutation in S209 codon generated a new NarI restriction site (underlined) into exon 8. (*C*) Southern blotting was performed using 5′ and 3′ specific probes on SacI-digested DNA isolated from ES cells or mouse tails to test for proper insertion/recombination of the targeting vector in the eIF4E locus on chromosome 3. Lanes 1 and 6, ES cells heterozygous for the KI mutation; lanes 2 and 4, WT mice; lanes 3 and 5, KI heterozygote mice. For a WT allele, 5′ and 3′ probes hybridize to a 13.7-kb fragment. For a KI allele, 5′ probe hybridizes to a 8.4-kb fragment and 3′ probe hybridizes to a 10.5-kb fragment. (*D*) Digestion of a PCR product amplified from oligonucleotides flanking the S209 codon shows that only the recombined allele containing the S209A mutation is cut by NarI. PCR genotyping with primer 1 and 2 produced a 1.1-kb product [lane 1 (WT mouse) and lane 3 (KI heterozygote mouse)]. Digestion of the 1.1-kb PCR product from the KI allele with NarI yielded 0.7- and 0.4-kb bands (compare lane 4 vs. lane 2). (*E*) Lanes 1 through 3 show PCR products obtained using primers 3 and 4 flanking the Frt sites, confirming the removal of the TK-Neo cassette. Lane 1, homozygous KI mouse; lane 2, WT mouse; lane 3, heterozygote KI mouse.

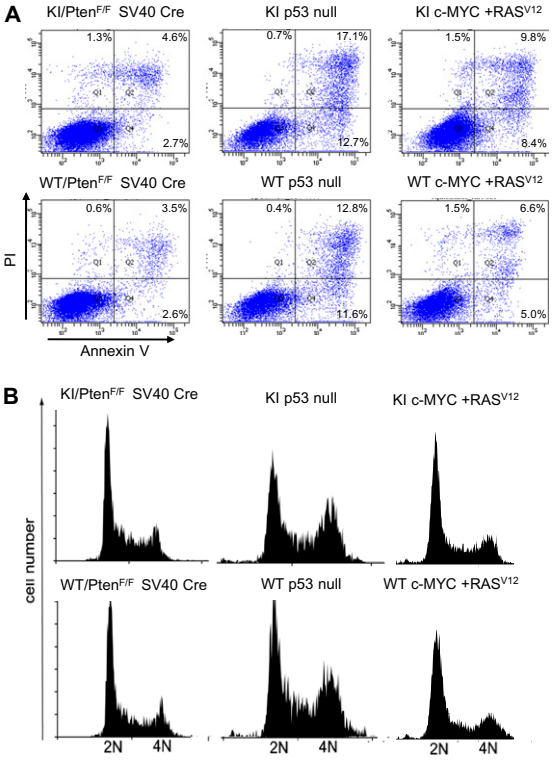

C

Cell line	Sub G0	G0/G1	S phase	G2/M
KI/PTEN$^{F/F}$ SV40 Cre	3.92%	46.11%	21.17%	25.35%
WT/PTEN$^{F/F}$ SV40 Cre	1.68%	46.35%	22.79%	24.76%
KI p53 null	1.10%	41.72%	14.56%	38.94%
WT p53 null	2.09%	43.12%	15.89%	35.41%
KI c-MYC+RAS^{V12}	1.38%	56.09%	22.17%	18.35%
WT c-MYC+RAS ^{V12}	1.04%	57.05%	19.79%	18.80%

Fig. S2. Apoptosis and cell cycle analysis of immortalized and transformed WT and KI MEFs. (*A*) Detection of apoptotic cells by Annexin V/PI costaining. MEFs of the indicated genotype (2×10^5 cells) were grown for 24 h, collected, and analyzed by flow cytometry to detect Annexin V and PI staining. (*B*) Cell cycle analysis. MEFs of the indicated genotype (2×10^5 cells) were grown for 24 h, collected, and analyzed by flow cytometry to detect DAPI staining. (*C*) Percentage of cells in each phase of the cell cycle.

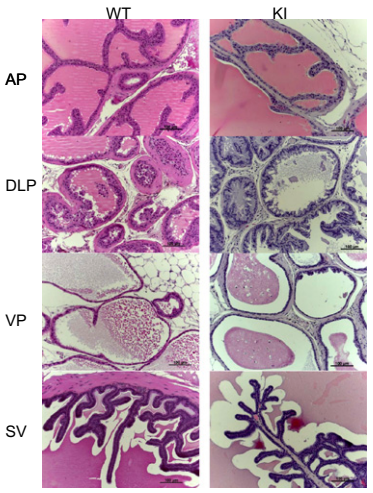

Fig. S3. Representative microphotographs of the seminal vesicle (SV) and of the ventral (VP), anterior (AP), and DLP lobes from the prostate of WT and KI mice. (Scale bar: 100 μm.)

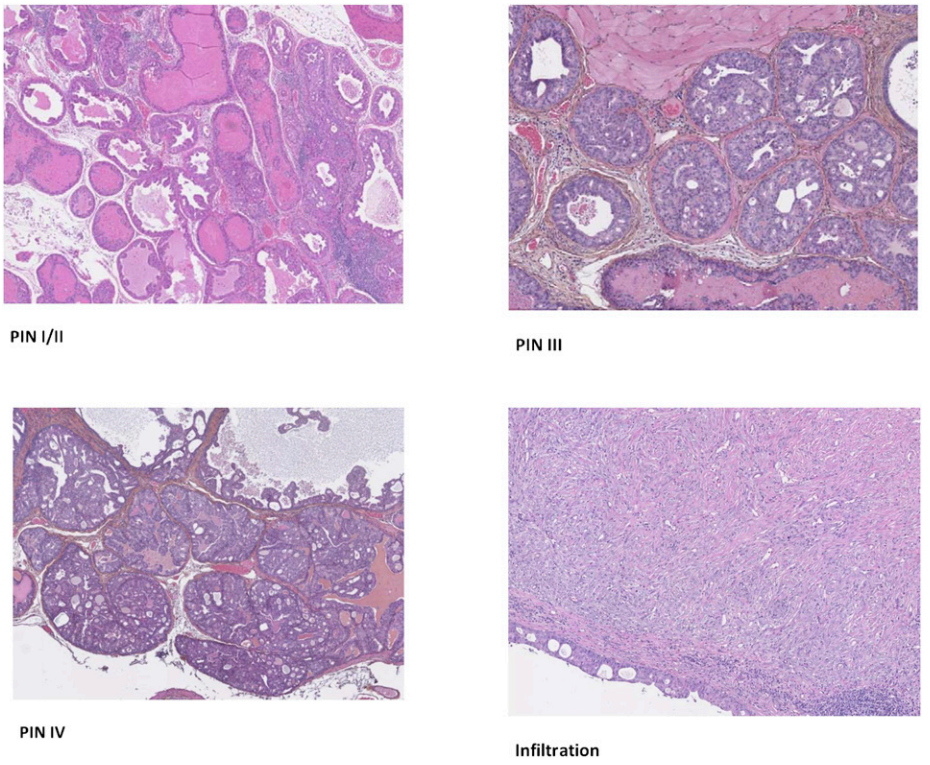

Fig. S4. Representative microphotographs of the lesions observed and their grading from PIN I to PIN IV and invasive.

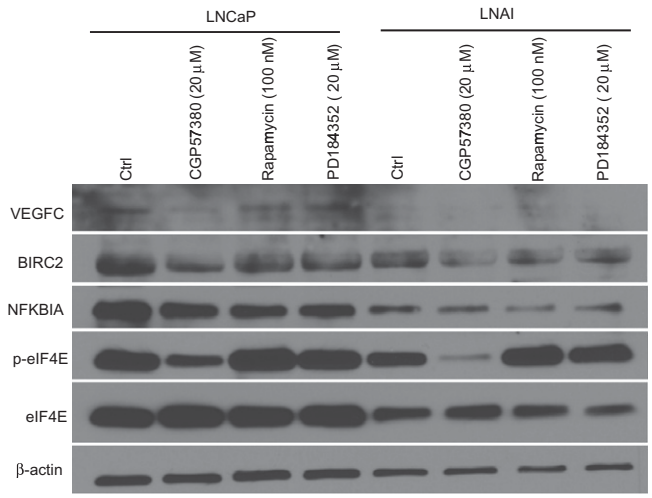

Fig. S5. LNCaP and LNAI prostate cancer cells were serum starved for 16 h. Cells were refed with 10% serum 1 h after the addition of the indicated inhibitors. Two hours after serum addition, cells were lysed and proteins were resolved by SDS/PAGE followed by Western blot analysis to detect the indicated proteins.

Table S1. Age of mice at the time they were euthanized

Type	5 mo	6 mo	7 mo	Median age, wk
WT/cPten$^{F/F}$	5	2	0	20
KI/cPten$^{F/F}$	2	3	2	25

Table S2. List of mRNAs more actively translated in WT compared with KI MEFs

Gene symbol	Fold change	Description
8430410K20Rik	5.09	RIKEN cDNA 8430410K20 gene
Enpp2	4.41	Ectonucleotide pyrophosphatase/phosphodiesterase 2
Dcn	4.05	Decorin
Birc2	3.54	Baculoviral IAP repeat-containing 2
Casp4	3.51	Caspase 4, apoptosis-related cysteine peptidase
Ccl7	3.36	Chemokine (C-C motif) ligand 7
Upp1	2.80	Uridine phosphorylase 1
C3	2.72	Complement component 3
Cbr3	2.51	Carbonyl reductase 3
Mmp3	2.46	Matrix metallopeptidase 3
Ccl2	2.42	Chemokine (C-C motif) ligand 2
Slco4a1	2.39	Solute carrier organic anion transporter family, member 4a1
Cd82	2.29	CD82 antigen
Adh7	2.16	Alcohol dehydrogenase 7 (class IV), mu or sigma polypeptide
Lxn	2.15	Latexin
Cyp1b1	2.12	Cytochrome P450, family 1, subfamily b, polypeptide 1
Serpina3g	2.07	Serine (or cysteine) peptidase inhibitor, clade A, member 3G
Sfrs3	2.03	Splicing factor, arginine/serine-rich 3 (SRp20)
Thbs2	2.02	Thrombospondin 2
Nfkbia	1.92	Nuclear factor of κ-light polypeptide gene enhancer in B-cells inhibitor, alpha
Prl2c4	1.92	Prolactin family 2, subfamily c, member 4
Zfp36l1	1.79	Zinc finger protein 36, C3H type-like 1
Bxdc1	1.74	Brix domain containing 1
Vegfc	1.73	Vascular endothelial growth factor C
Ssca1	1.71	Sjogren syndrome/scleroderma autoantigen 1 homologue (human)
Plk2	1.70	Polo-like kinase 2 (Drosophila)
Prl2c3	1.67	Prolactin family 2, subfamily c, member 3
Arhgef3	1.66	Rho guanine nucleotide exchange factor (GEF) 3
Ccl9	1.61	Chemokine (C-C motif) ligand 9
Dcun1d5	1.58	DCN1, defective in cullin neddylation 1, domain containing 5 (*Saccharomyces cerevisiae*)
Pdgfra	1.57	Platelet derived growth factor receptor, alpha polypeptide
Slc24a3	1.56	Solute carrier family 24 (sodium/potassium/calcium exchanger), member 3
Mtvr2	1.55	Mammary tumor virus receptor 2
Mmp9	1.53	Matrix metallopeptidase 9
Rbmx	1.51	RNA binding motif protein, X chromosome

Table S3. Correlation analysis among pERK, pAKT, MMP3, peIF4E, and eIF4E in prostate cancer tumor tissues

Comparison	pERK	pAKT	MMP3	peIF4E	eIF4E
pERK					
Correlation coefficient	1	0.258*	0.006	0.266*	0.244
Significance	–	0.046	0.966	0.038	0.058
pAKT					
Correlation coefficient	0.258*	1	0.11	0.321*	0.395**
Significance	0.046	–	0.399	0.011	0.002
MMP3					
Correlation coefficient	0.006	0.11	1	0.396**	0.524**
Significance	0.966	0.399	–	0.001	<0.001
peIF4E					
Correlation coefficient	0.266*	0.321*	0.396**	1	0.550**
Significance	0.038	0.011	0.001	–	0
eIF4E					
Correlation coefficient	0.244	0.395**	0.524**	0.550**	1
Significance	0.058	0.002	<0.001	<0.001	–

Correlation is significant at the *0.05 level or **0.01 level (two-tailed *P* value). Correlation coefficient is the Spearman ρ.